ACS SENSORS

pubs.acs.org/acssensors Article

Electrophoretic Assembly of Antibody–Antigen Complexes Facilitates 1000 Times Improvement in the Limit of Detection of Serological Paper-Based Assay

Vasily G. Panferov, Nikita A. Ivanov, Davor Brinc, Anselmo Fabros, and Sergey N. Krylov*

Cite This: *ACS Sens.* 2023, 8, 1792–1798 Read Online

ACCESS | Metrics & More | Article Recommendations | Supporting Information

ABSTRACT: Serological assays detect the presence of specific antibodies in blood. There are urgent and important applications for serological point-of-care (POC) assays. However, available detection methods are either insufficiently sensitive or too complex for POC settings. Here, we demonstrate that lateral flow immunoassay (LFIA), which is arguably the simplest universal molecular detection approach, can serve as a methodological platform for highly sensitive serological POC assays if combined with a simple, fast, and inexpensive electrophoretic step. In this work, we compared such electrophoretically driven LFIA (eLFIA) with conventional LFIA for the detection of immunoglobulins G against hepatitis B and C in serum. The limit of detection of eLFIA was proven to be 1000 times lower than that of conventional LFIA and sufficiently low to support clinical serological tests. eLFIA takes less than 10 min, requires only a minor accessory powered by a small 9 V battery, and can be performed by an untrained person in the POC environment using a 3 μL specimen of finger-prick capillary blood.

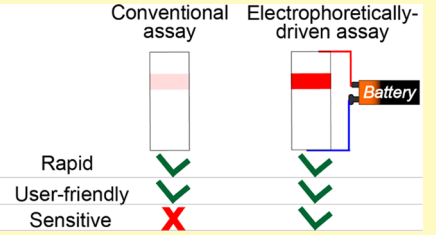

KEYWORDS: *immunoglobulins G, lateral flow immunoassay, pathogens, serological assays*

Serological assays encompass methods for the detection of antibodies against a specific antigen in blood.[1] The presence of antigen-specific immunoglobulins G (IgG_{sp}) is indicative of the organism's previous exposure to the antigen.[2] Serological point-of-care (POC) assays are needed to effectively assess the immune response of individuals to vaccination and the infection fatality risk of pathogens for the population.[3,4] They are also pivotal for monitoring the spread of zoonotic pathogens, such as coronavirus and monkeypox virus, in wildlife and domestic animals.[5−9]

The gold standard in serological testing is multistage instrumental assays, among which enzyme-linked immunosorbent assay (ELISA) is the most widely used one.[10] ELISA is highly sensitive but not suitable for POC applications since it requires expensive stationary equipment, takes a long time, and must be performed by trained personnel.[11] Moreover, it is not accessible to users in large areas of developing countries and may not be economically feasible for some urgent uses, such as monitoring pathogen spread in wildlife and domestic animals, even in developed countries.

There are examples of serological POC assays, but they may be ineffective when disease diagnosis requires a very low limit of detection (LOD).[12,13] Some serological POC assays have been recently proposed for samples with low concentrations of IgG_{sp}, but despite being aimed at obvious and urgent applications, they found little practical use owing mainly to their technical limitations.[14−17] Thus, finding a suitable approach for highly sensitive POC serological assays is both an important and pressing task for analytical chemists.[18]

Lateral flow immunoassay (LFIA)—which uses test strips assembled of multiple membranes preloaded with dried reagents—is arguably the simplest and least expensive approach for POC molecular diagnostics. A conventional one-step LFIA is widely used for detecting various types of molecules;[19,20] however, it can hardly facilitate the sensitive detection of IgG_{sp} in serological testing. The main reason for this constraint is the competition between a small amount of IgG_{sp} and a large amount of background IgG (IgG_{bg}) against other antigens for the binding to a limited amount of IgG-binding protein.[21] By examining the technological concepts of the conventional serological LFIA, we aim to highlight its fundamental limitations.

In conventional serological LFIA, the antigen (Ag) is immobilized in the test zone (Figure 1). An IgG-binding protein (antispecies antibody, bacterial protein A, or bacterial protein G) is conjugated with red-colored gold nanoparticles (GNPs), serving as labels for visual detection. Because conventionally used spherical GNP with a diameter of 20–40 nm is much larger than the protein, every particle has multiple molecules of the protein immobilized on its surface,

Received: January 19, 2023
Accepted: March 17, 2023
Published: March 29, 2023

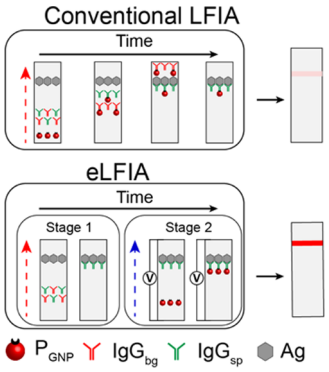

Figure 1. Schematics of serological tests utilizing conventional LFIA and electrophoretically driven LFIA (eLFIA). Both assays use test strips with immobilized Ag in the test zone. In conventional LFIA, the competition of IgG_{sp} with IgG_{bg} for binding with a limited amount of P_{GNP} leads to a low amount of labeled immunocomplexes in the test zone, resulting in low coloration of the test zone. The red-dotted arrow shows the direction of the sample flow. In eLFIA, in stage 1, all IgG_{sp} are captured by the Ag, while IgG_{bg} antibodies are washed away by capillary action. Then, in stage 2, P_{GNP} is moved by electrophoresis to the test zone, where it reacts with IgG_{sp} in the absence of competition with IgG_{bg} leading to a large amount of GNP-labeled immunocomplexes, resulting in high coloration of the test zone. The blue-dotted arrow shows the direction of P_{GNP} electromigration.

but for convenience, we still use the term "GNP-labeled protein" (P_{GNP}). P_{GNP} is present in a mobilizable form on the membrane and is typically positioned between the sample loading zone and the test zone.

A liquid sample—unavoidably containing a large amount of IgG_{bg} and a much smaller amount (if any) of IgG_{sp}—is deposited on a dry strip and is carried laterally along the membranes by capillary action. First, it reaches the zone with dried P_{GNP} and rehydrates it, hence initiating the binding of all IgG in the sample to a limited amount of P_{GNP} preloaded on the test strip. Because the amount of P_{GNP} is typically much smaller than the total amount of IgG, P_{GNP} can bind only a small fraction (less than 1%) of total IgG in the sample.[21,22] Accordingly, only a small fraction of IgG_{sp} forms complexes with P_{GNP} (P_{GNP}–IgG_{sp}), whereas the majority of IgG_{sp} remains unbound.[21] Further, the sample is moved by capillary action toward the test zone where IgG_{sp} is captured by Ag, while IgG_{bg} passes the test zone. Since only a small fraction of IgG_{sp} is bound to P_{GNP}, only a small amount of GNP-containing ternary immunocomplexes P_{GNP}–IgG_{sp}–Ag are formed in the test zone. As a result, low coloration intensity is observed, drastically affecting the assay's LOD and diagnostic sensitivity.[23,24]

It is important to emphasize that the problem of the excess of total IgG over P_{GNP} cannot be solved by increasing the IgG-binding capacity of P_{GNP} preloaded on the test strip. On the one hand, loading a greater number of nanoparticles inevitably results in the growth of nonspecific signal in the test zone leading to false-positive results.[25] On the other hand, the increase of IgG-binding activity of GNP by conjugating more IgG-binding protein per nanoparticle is impossible due to the limited protein-sorption capacity of GNP.[26] As a result of these confines, most of IgG_{sp} in conventional serological LFIA remains unbound to P_{GNP}.[21] A few enhancement and optimization strategies for serological LFIA have been proposed, but they greatly complicate the procedure and/or do not achieve the required LOD and, thus, the needed diagnostic sensitivity.[27−31]

To increase the sensitivity of serological LFIA, one needs to find a means of preventing the competition between IgG_{sp} and IgG_{bg} for binding to P_{GNP}. Preventing this competition would facilitate a significantly higher amount of P_{GNP}–IgG_{sp}–Ag formed in the test zone and, hence, its greater level of coloration. Furthermore, preventing this competition would presumably enable a universal approach for serological LFIA for any type of antigen.

This work was inspired by our insight that the removal of IgG_{bg} followed by the assembly of ternary immunocomplexes P_{GNP}–IgG_{sp}–Ag (thus preventing the assembly of P_{GNP}–IgG_{bg}–Ag) could be achieved using electrophoretically driven LFIA (eLFIA). Electrophoresis has been successfully utilized in instrumentation-based immunoassays.[32,33] It has also been productively used on paper-based devices for biomolecular separation, concentration of affinity complexes, and enhancement of sensitivity.[34−37] In our recent work, we successfully utilized eLFIA for the layer-by-layer assembly of GNP aggregates leading to a greatly enhanced coloration of the test zone in a rapid antigen test.[38] Here, we intended to use eLFIA for moving the liquid controllably through the test strip to prevent the competition between IgG_{sp} and IgG_{bg} for binding with P_{GNP} and thus facilitate a large number of labeled complexes in the test zone.

MATERIALS AND METHODS

The detailed description of all reagents, synthesis of GNP and P_{GNP}, measuring the temperature of the test strips for eLFIA, and the determination of the effect of storage of test strips between the two stages of eLFIA is reported in the Supporting Information.

Assembly of Test Strips. The reagents were dispensed on the nitrocellulose membrane using a syringe pump "Pump 11 Elite" from Harvard Instruments (Holliston, Massachusetts) at a rate of 1.5 μL/cm. Hepatitis B surface antigen (0.5 mg/mL, 20 mM sodium phosphate buffer, pH 7.5) and a cocktail of recombinant hepatitis C proteins (0.5 mg/mL, 20 mM sodium phosphate buffer, pH 7.5) were dispensed as two separate test lines. For eLFIA, the dried conjugate was not included in the test strip. Cellulose membranes (sample and adsorbing membranes) were glued to the nitrocellulose membrane. The membranes were dried at 30 °C and humidity less than 20% for 24 h. After drying, the membranes were cut manually to 4 mm wide test strips and stored at room temperature and humidity of less than 10%. For conventional LFIA, a dried conjugate of GNP with protein G was included in the test strip. The conjugate was diluted with a buffer (20 mM tris–acetate, pH 7.6, 1% bovine serum albumin, 0.1% Triton X-100, 0.5% sucrose, and 0.05% sodium azide) to $OD_{520\,nm}$ = 0.8 measured in a cuvette with a 1 mm optical path length. The fiberglass membrane was soaked with the conjugate (2.5 μL per mm) and dried at room temperature and humidity of less than 20% for 12 h. Cellulose and fiberglass membranes were glued to the nitrocellulose membrane. The membranes were dried, cut, and stored as described above.

Fabrication of Holder for Electrophoresis. The holder of test strips for electrophoresis was fabricated of poly(methyl methacrylate) plastic. The holder components were machined using a MODELA MDX-540 Benchtop Milling Machine from Roland DGA (Irvine, California). Platinum wire electrodes (0.25 mm) were inserted into the buffer reservoirs. The electrophoresis driving circuit is powered by a generic 9 V battery. The battery is connected to a step-up DC–DC transformer through a 10 kΩ generic potentiometer that acts as an adjustable voltage divider (Figure S5B). The electrophoresis voltage output can be controlled by adjusting the potentiometer. The step-up circuit is assembled on a solderable mini-breadboard (SparkFun, PRT-12702) using a generic 63/37 Sn–Pb solder alloy.

https://doi.org/10.1021/acssensors.3c00130
ACS Sens. 2023, 8, 1792−1798

Assay Performance. For the proof-of-concept experiments, the conventional and eLFIA were performed in human serum and capillary blood spiked with monoclonal antibodies to hepatitis B surface antigen. Spiked serum was diluted 10 times by 50 mM sodium borate buffer, pH 8.0, containing 0.08% of 2-hydroxyethyl cellulose (HEC, MW 380 kDa) and 0.1% of sodium dodecyl sulfate. Capillary blood was diluted 50 times using the same buffer with the addition of ethylenediaminetetraacetic acid (final concentration 2 mg/mL).

For conventional LFIA, test strips (with dried P_{GNP}) were vertically immersed into the wells of the 96-well plate. The analyzed sample (100 μL) was added to each well and incubated with the test strips for 5 min. After 5 min of incubation, the test strips were scanned using an Epson V600 scanner with a resolution of 3200 dpi. The digital images were used for the quantification of test zone color intensity using TotalLab TL120 from Nonlinear Dynamics (Newcastle, U.K.). Calibration plots were obtained as a function of the measured colorimetric signals (relative units, RU) vs the spiked concentrations of IgG using OriginPro 2021 from OriginLab corporation (Northampton, Massachusetts). Following the IUPAC recommendations, the limit of detection (LOD) of the assay with a 99% confidence interval was determined as the IgG concentration that provides the colorimetric signal of the test zone higher than a value of blank (nonspiked samples, A_{blank}) plus three standard deviations of A_{blank} (SD_{blank}), i.e., LOD = A_{blank} + $3SD_{blank}$.[39]

For eLFIA, test strips (without dried P_{GNP}) were used. The test strips were incubated with the samples as described above. After a 3 min incubation with the sample (shortened incubation because of the absence of P_{GNP}), the test strips were inserted into the holder for electrophoresis. The plastic holder holds the ends of the test strips into two wells containing the running buffer (the same as used for the LFIA) and Pt-wire electrodes. The running buffer was refreshed for each measurement. The P_{GNP} conjugate was diluted with the running buffer to OD_{520} = 0.5 measured in a cuvette with a 1 mm optical path length. The drop of P_{GNP} (2.0 μL) was applied onto the nitrocellulose membrane near the cathode. The voltage was applied using the voltage-amplifying circuit. After 3 min, the voltage was turned off, and the membranes were optically scanned as described above.

Clinical Validation. Serum samples were analyzed by testing laboratories in the Toronto General Hospital using Abbott chemiluminescent microparticle immunoassay Alinity i (Abbott Diagnostics, Abbott Park, Illinois) for the anti-HBs and anti-HCV antibodies. The sample was considered positive if anti-HBS was ≥10 IU/L and anti-HCV was ≥1 S/CO. In summary, 94 anti-HBs positive (anti-HBs in a range of 10−25,000 IU/L), 26 anti-HCV positive (anti-HCV in a range of 2−22 S/CO), 18 anti-HBs negative (anti-HBs below 10 IU/L), and 43 anti-HCV negative (anti-HCV below 1 S/CO) serum samples were used for validation. Each sample was tested at least in two replicates by the testing laboratories. The results of Abbott Alinity assay were accepted as a reference (i.e., true positive and true negative) for the comparison with conventional LFIA and eLFIA.

The performance of conventional LFIA and eLFIA is described in the Assay Performance section. The second stage of eLFIA (electromigration of P_{GNP}) was performed within 24 h after completion of the first step unless otherwise stated. The sensitivity of LFIAs was determined as the ratio of the number of true-positive samples (measured with Abbott Alinity i) to the number of positive samples measured by LFIA.

RESULTS AND DISCUSSION

Concept of eLFIA. The concept of the proposed serological eLFIA is as follows (Figure 1). In stage 1, a serum sample is added to the test strip with Ag immobilized in the test zone but without P_{GNP} on the strip. Similar to the conventional LFIA, the sample migrates through the test strip driven by capillary action, facilitating the formation of only IgG_{sp}−Ag immunocomplexes in the test zone and the removal of IgG_{bg}, which pass the test zone. After the completion of stage 1 (3 min), stage 2, which includes the electrophoretic migration of P_{GNP}, is performed. Electrophoresis is used as a driving force instead of capillary action because the latter is negligible on wet membranes. Driven by electrophoresis, P_{GNP} migrates through the test zone, enabling the formation of GNP-labeled ternary immunocomplexes P_{GNP}−IgG_{sp}−Ag. As all IgG_{bg} were washed away in stage 1, they do not compete for binding to P_{GNP} in stage 2. Thus, a large quantity of P_{GNP}−IgG_{sp}−Ag is formed in the test zone, resulting in its higher coloration. In addition, during electrophoresis-driven migration, P_{GNP} is focused by electrostacking in a narrow band with higher local concentration, thus enabling favorable kinetic conditions for faster binding.[38] In summary, the proposed serological eLFIA is expected to facilitate the decrease in LOD (and thus increase in sensitivity) through (i) preventing the competition between IgG_{sp} and IgG_{gb} for binding to P_{GNP} and (ii) more favorable kinetic conditions for the binding of P_{GNP} to the dual immunocomplexes IgG_{sp}−Ag.

In this proof-of-concept study for serological eLFIA, we used hepatitis B surface antigen as Ag and monoclonal antibodies against this antigen as IgG_{sp}. We synthesized and characterized P_{GNP}—a conjugate of GNP, bearing a negative charge, with the IgG-binding protein G (Figure S1). Preoptimized conditions for electromigration of P_{GNP} were used.[38] Electrophoresis unavoidably leads to Joule heating, which can cause denaturation of the immunocomplexes. We studied the dependence of strip temperature on the applied voltage with a thermal camera and used the voltage that ensured that the temperature did not exceed 40 °C (Figure S2).

Analytical Performance of LFIA and eLFIA. To show the impact of the electrophoretic step on the LOD of eLFIA, we spiked IgG_{sp} into the serum. We compared the performance of eLFIA (Figure 2A) to that of conventional LFIA (Figure 2B) in IgG_{sp}-spiked serum, with the goal of confirming that the removal of IgG_{bg} benefits the LOD. We also compared eLFIA (Figure 2A) in IgG_{sp}-spiked serum to conventional LFIA in buffer (Figure 2C) in order to prove the benefits of more favorable kinetic conditions for binding between P_{GNP} and the dual immunocomplexes IgG_{sp}−Ag.

The results of eLFIA with IgG_{sp}-spiked serum (Figure 2A,B) established that eLFIA, in comparison to conventional LFIA, facilitated much greater coloration of the test zone and 3 orders of magnitude reduction in LOD (from 625 to 0.6 ng/mL). By comparing LOD values of conventional LFIA in serum (625 ng/mL; Figure 2B) and in the buffer (4.9 ng/mL; Figure 2C), we confirmed the drastic interfering effect of IgG_{bg} in conventional serological LFIA. By comparing two LFIAs without interference from IgG_{bg}, i.e., eLFIA in spiked serum (Figure 2A) and conventional LFIA in a buffer (Figure 2C), we confirmed that the electrophoretic step by itself results in an order-of-magnitude reduction in LOD (from 4.9 to 0.6 ng/mL). This improvement in LOD can be explained by the electrostacking of P_{GNP}.[40] As a result of electrostacking, a higher local concentration of P_{GNP} is formed, facilitating more kinetically favorable conditions for binding with IgG_{sp}−Ag in the test zone.

With concentrations of the spiked IgG_{sp} above 1000 ng/mL, the coloration intensity in the test zone for LFIA in the buffer significantly declines (Figure 2D). The reason for this decrease is the blocking of Ag in the test zone by the excess of IgG_{sp} unbound to P_{GNP}. As a result of binding of the excess of P_{GNP}-unbound IgG_{sp} to the Ag, the amount of Ag available for binding to P_{GNP}-bound IgG_{sp} is drastically decreased. Less of

https://doi.org/10.1021/acssensors.3c00130
ACS Sens. 2023, 8, 1792−1798

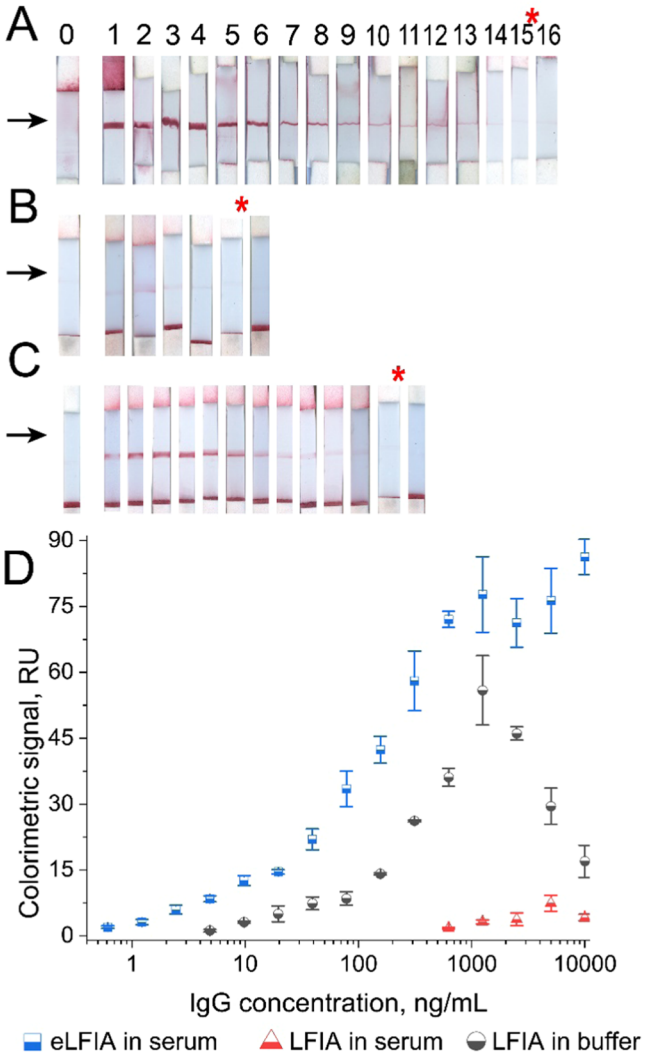

Figure 2. Detection of IgG to hepatitis B antigen with various formats of LFIA. (A) The test strips after eLFIA in serum. (B) The test strips after conventional LFIA in serum. (C) The test strips after conventional LFIA in a buffer with no IgG_{bg}. The numbers above the test strips correspond to concentrations of IgG (ng/mL) obtained by serial dilution and rounded: 0, blank; 1, 10000; 2, 5000; 3, 2500; 4, 1250; 5, 625; 6, 313; 7, 156; 8, 78; 9, 39; 10, 20; 11, 9.8; 12, 4.9; 13, 2.4; 14, 1.2; 15, 0.6; and 16, 0.3. Red asterisks show the LOD values for (A) (0.6 ng/mL), (B) (625 ng/mL), and (C) (4.9 ng/mL). The black arrows show the position of the test zones. (D) Colorimetric signals of the test zone on the test strips shown in panels (A)−(C) vs IgG concentrations in serum, n = 3.

P_{GNP}−IgG_{sp} is bound in the test zone leading to a lower level of the labeled ternary immunocomplexes P_{GNP}−IgG_{sp}−Ag. For eLFIA, we did not observe this effect because the ternary immunocomplexes are assembled consequently: first, IgG_{sp} reacts with Ag forming IgG_{sp}−Ag in the test zone and then P_{GNP} is introduced for the labeling of IgG_{sp}−Ag. In this case, there is no blocking of Ag by the excess of unlabeled IgG_{sp}. The coloration is roughly proportional to the amount of ternary immunocomplexes and is limited only by the amount of Ag immobilized in the test zone.

Clinical Validation of LFIA and eLFIA. We then validated both conventional LFIA and eLFIA using clinical samples (Figure S3). Serum samples containing anti-hepatitis B antibodies (anti-HBs) (16−25000 IU/L, 94 samples), anti-hepatitis C antibodies (anti-HCV) (2.6−22 S/CO, 26 samples), and serum samples from healthy patients (anti-HBS < 10 IU/L; anti-HCV < 1 S/CO, 61 samples in total) were used for the assay validation. The colorimetric signals for eLFIA were 5−50 times higher than for conventional LFIA (Figure S3). As a result, a moderate diagnostic sensitivity typical for conventional serological LFIA relative to the instrumental test used clinically (75% for anti-HBs, 65% for anti-HCV) was drastically improved in eLFIA (to 98% for anti-HBs and to 96% for anti-HCV; Table S1). Icterus (Figure S3; samples # 60 and 76) and hemolysis (<10 mg/mL of hemoglobin) do not interfere with the visual registration of colored GNP in the test zone (Figure S4). Using as references the quantities of anti-HBs in clinical samples determined with an instrumental assay (a chemiluminescent microparticle immunoassay Abbot Alinity i Anti-HBs), we confirmed that the LOD of eLFIA (≈10 IU/L) was sufficient for highly sensitive serological testing of patients after immunization against hepatitis B (Figure S5). The LOD of our serological eLFIA meets WHO recommendations.[41−43]

Applicability of eLFIA for POC Settings. Importantly, serological eLFIA satisfies the simplicity criterion of POC tests, which demands that no sophisticated instrumentation be used.[44] Stage 2 of eLFIA requires only a minor electrophoretic accessory (Figure 3), which can be easily used by an untrained individual.

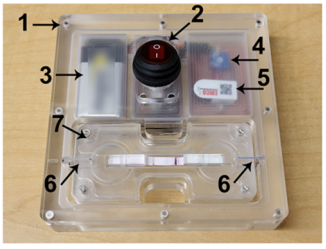

Figure 3. Assembled accessory for eLFIA. The major components include magnetic fasteners (1), on/off switch (2), 9 V battery (3), voltage control potentiometer (4), DC−DC step-up transformer (5), platinum electrodes (6), and test strip holder (7). A 9 V battery is used as a power supply; the circuit transforms 9 V from the battery to 200 V applied to the test strip.

Furthermore, this accessory does not require a power outlet as electrophoretic migration can be driven by a generic 9 V alkaline battery (the circuit diagram of the accessory is shown in Figure S6). The estimated cost of the assembled disposable device is less than $20, while the electronics is the most expensive part (Table S2). Considering that the accessory is reusable, it does not contribute significantly to the testing cost and keeps LFIA in the paradigm of an affordable method.

We also considered the potential use of eLFIA when the electrophoretic accessory is not available. In this case, stage 1 (Figure 1) is performed at the point of testing, and test strips are then stored until the accessory becomes available. To facilitate this assay format, we studied the effects of temperature, humidity, and strip storage time between the two stages on the assay results. We found that under the optimized storage conditions (temperature < 30 °C, humidity < 10%), the signal in the test zone was stable for 3 weeks (Figure S7). However, when the test strips were stored at a very high temperature of 55 °C, the signal was stable only for 6 days (Figure S8). Thus, the use of eLFIA in a very hot

https://doi.org/10.1021/acssensors.3c00130
ACS Sens. 2023, 8, 1792−1798

environment requires that (i) strips not be stored at an ambient temperature for longer than a week and (ii) the delay between stages 1 or 2 does not exceed a week. Overall, our results suggest high stability of eLFIA and its applicability to serological testing in rural and remote areas for the screening of immunity, disease prevalence, and diagnostics.

Finally, we evaluated the applicability of eLFIA to whole capillary blood (a lay user can safely obtain capillary blood in nonlaboratory conditions by finger-prick using a lancet pen). We found that eLFIA requires only 3 μL of capillary blood, which is diluted by a factor of approximately 30 with the electrophoresis running buffer before sampling on the strip. We confirmed the low LOD of 0.4 ng/mL (similar to LOD = 0.6 ng/mL of the serum assay) for eLFIA in diluted capillary blood (Figure S9). Considering typical concentrations of IgG_{sp} after infection or immunization, the sensitivity of eLFIA, even after the dilution with the buffer, may be sufficient for the serological testing in many types of IgG_{sp}.[45,46]

CONCLUSIONS

To summarize, we introduced serological point-of-care electrophoretically enhanced lateral flow immunoassay for highly sensitive detection of antibodies. The high sensitivity was achieved by preventing the competition between specific and background antibodies for binding to the nanosized label. This prevention was achieved via electrokinetically driven delivery of the label after the antigen−antibody binding in the test zone. The developed method was applied to the detection of antibodies against hepatitis B and C. We confirmed the applicability of the assay to serum and capillary blood with a diagnostic sensitivity of 98% for hepatitis B and 96% for hepatitis C. The assay can be performed in nonlaboratory settings using an inexpensive plastic accessory and a simple circuit powered by a generic 9 V battery. These results confirm that the proposed eLFIA matches the REASSURED criteria and can be applied for serological testing of humans as well as domestic and wildlife animals. The further advancement of eLFIA will necessarily include the multiplexing of assays. Targets for serological and antigen tests are often present together. For example, the satellite hepatitis D virus co-occurs with the hepatitis B virus.[47] Drug users often contract multiple blood-transmitted infections such as hepatitis B and C, human immunodeficiency virus, and human T-lymphotropic virus.[48] Multiple antibodies specific to different allergens must be detected simultaneously when screening for allergies.[49]

ASSOCIATED CONTENT

Supporting Information

The Supporting Information is available free of charge at https://pubs.acs.org/doi/10.1021/acssensors.3c00130.

Materials and methods; and supporting figures and tables (PDF)

AUTHOR INFORMATION

Corresponding Author

Sergey N. Krylov − *Department of Chemistry, York University, Toronto, Ontario M3J 1P3, Canada;* orcid.org/0000-0003-3270-2130; Email: skrylov@yorku.ca

Authors

Vasily G. Panferov − *Department of Chemistry, York University, Toronto, Ontario M3J 1P3, Canada; A.N. Bach Institute of Biochemistry, Federal Research Centre "Fundamentals of Biotechnology", Russian Academy of Sciences, Moscow 119071, Russia;* orcid.org/0000-0002-4057-7248

Nikita A. Ivanov − *Department of Chemistry, York University, Toronto, Ontario M3J 1P3, Canada;* orcid.org/0000-0002-0842-6626

Davor Brinc − *Toronto General Hospital, University Health Network, Toronto, Ontario M5G 2C4, Canada*

Anselmo Fabros − *Toronto General Hospital, University Health Network, Toronto, Ontario M5G 2C4, Canada*

Complete contact information is available at: https://pubs.acs.org/10.1021/acssensors.3c00130

Author Contributions

V.G.P. conceptualized and implemented the project and wrote the manuscript. N.A.I. provided technical ideas and contributed to experimental investigation. D.B. and A.F. validated the results. S.N.K. conceived and guided the project and wrote the manuscript.

Notes

The authors declare no competing financial interest.

ACKNOWLEDGMENTS

This work was supported by the NSERC grant (STPG-P 521331-2018) and the Collaborative Interdisciplinary Research Cluster "Technologies for Identification and Control of Infectious Diseases at York University" to S.N.K. as well as by Banting postdoctoral fellowship (appl. no. 454188) and the Ministry of Science and Higher Education of the Russian Federation to V.G.P.

REFERENCES

(1) Turgeon, M. *Immunology and Serology in Laboratory Medicine*; Butter Wroth-Heinemann Ltd., 2014.

(2) Liu, G.; Rusling, J. F. COVID-19 Antibody Tests and Their Limitations. *ACS Sens.* **2021**, *6*, 593−612.

(3) Tong, H.; Cao, C.; You, M.; Han, S.; Liu, Z.; Xiao, Y.; He, W.; Liu, C.; Peng, P.; Xue, Z.; Gong, Y.; Yao, C.; Xu, F. Artificial Intelligence-Assisted Colorimetric Lateral Flow Immunoassay for Sensitive and Quantitative Detection of COVID-19 Neutralizing Antibody. *Biosens. Bioelectron.* **2022**, *213*, No. 114449.

(4) Sorensen, R. J. D.; Barber, R. M.; et al. Variation in the COVID-19 Infection−Fatality Ratio by Age, Time, and Geography during the Pre-Vaccine Era: A Systematic Analysis. *Lancet* **2022**, *399*, 1469−1488.

(5) Barshevskaya, L. V.; Sotnikov, D. V.; Zherdev, A. V.; Khassenov, B. B.; Baltin, K. K.; Eskendirova, S. Z.; Mukanov, K. K.; Mukantayev, K. K.; Dzantiev, B. B. Triple Immunochromatographic System for Simultaneous Serodiagnosis of Bovine Brucellosis, Tuberculosis, and Leukemia. *Biosensors* **2019**, *9*, No. 115.

(6) Sastre, P.; Gallardo, C.; Monedero, A.; Ruiz, T.; Arias, M.; Sanz, A.; Rueda, P. Development of a Novel Lateral Flow Assay for Detection of African Swine Fever in Blood. *BMC Vet. Res.* **2016**, *12*, No. 206.

(7) Nakhaie, M.; Arefinia, N.; Charostad, J.; Bashash, D.; Haji Abdolvahab, M.; Zarei, M. Monkeypox Virus Diagnosis and Laboratory Testing. *Rev. Med. Virol.* **2022**, *33*, No. e2404.

(8) Chan, F. H. M.; Ataide, R.; Richards, J. S.; Narh, C. A. Contrasting Epidemiology and Population Genetics of COVID-19 Infections Defined by Multilocus Genotypes in SARS-CoV-2 Genomes Sampled Globally. *Viruses* **2022**, *14*, No. 1434.

(9) Carlson, C. J.; Farrell, M. J.; Grange, Z.; Han, B. A.; Mollentze, N.; Phelan, A. L.; Rasmussen, A. L.; Albery, G. F.; Bett, B.; Brett-Major, D. M.; Cohen, L. E.; Dallas, T.; Eskew, E. A.; Fagre, A. C.; Forbes, K. M.; Gibb, R.; Halabi, S.; Hammer, C. C.; Katz, R.; Kindrachuk, J.; Muylaert, R. L.; Nutter, F. B.; Ogola, J.; Olival, K. J.; Rourke, M.; Ryan, S. J.; Ross, N.; Seifert, S. N.; Sironen, T.; Standley, C. J.; Taylor, K.; Venter, M.; Webala, P. W. The Future of Zoonotic Risk Prediction. *Philos. Trans. R. Soc., B* **2021**, *376*, No. 20200358.
(10) Ravi, N.; Cortade, D. L.; Ng, E.; Wang, S. X. Diagnostics for SARS-CoV-2 Detection: A Comprehensive Review of the FDA-EUA COVID-19 Testing Landscape. *Biosens. Bioelectron.* **2020**, *165*, No. 112454.
(11) Toropov, N.; Osborne, E.; Joshi, L. T.; Davidson, J.; Morgan, C.; Page, J.; Pepperell, J.; Vollmer, F. SARS-CoV-2 Tests: Bridging the Gap between Laboratory Sensors and Clinical Applications. *ACS Sens.* **2021**, *6*, 2815−2837.
(12) Laforgerie, E.; Boucher, B.; Ly, T. D.; Maisoneuve, L.; Izopet, J.; Delaugerre, C.; Simon, F. Sensitivity of 8 CE (European Community)-Approved Rapid Disposable Tests for Anti-HIV Antibody Detection during and after Seroconversion. *J. Virol. Methods* **2010**, *165*, 105−107.
(13) Steingart, K. R.; Henry, M.; Laal, S.; Hopewell, P. C.; Ramsay, A.; Menzies, D.; Cunningham, J.; Weldingh, K.; Pai, M. Commercial Serological Antibody Detection Tests for the Diagnosis of Pulmonary Tuberculosis: A Systematic Review. *PLoS Med.* **2007**, *4*, No. e202.
(14) Brangel, P.; Sobarzo, A.; Parolo, C.; Miller, B. S.; Howes, P. D.; Gelkop, S.; Lutwama, J. J.; Dye, J. M.; McKendry, R. A.; Lobel, L.; Stevens, M. M. A Serological Point-of-Care Test for the Detection of IgG Antibodies against Ebola Virus in Human Survivors. *ACS Nano* **2018**, *12*, 63−73.
(15) Zhu, M.; Zhang, J.; Cao, J.; Ma, J.; Li, X.; Shi, F. Ultrasensitive Dual-Color Rapid Lateral Flow Immunoassay via Gold Nanoparticles with Two Different Morphologies for the Serodiagnosis of Human Brucellosis. *Anal. Bioanal. Chem.* **2019**, *411*, 8033−8042.
(16) Cavalera, S.; Colitti, B.; Rosati, S.; Ferrara, G.; Bertolotti, L.; Nogarol, C.; Guiotto, C.; Cagnazzo, C.; Denina, M.; Fagioli, F.; Di Nardo, F.; Chiarello, M.; Baggiani, C.; Anfossi, L. A Multi-Target Lateral Flow Immunoassay Enabling the Specific and Sensitive Detection of Total Antibodies to SARS COV-2. *Talanta* **2021**, *223*, No. 121737.
(17) Zhang, Y.; Malekjahani, A.; Udugama, B. N.; Kadhiresan, P.; Chen, H.; Osborne, M.; Franz, M.; Kucera, M.; Plenderleith, S.; Yip, L.; Bader, G. D.; Tran, V.; Gubbay, J. B.; McGeer, A.; Mubareka, S.; Chan, W. C. W. Surveilling and Tracking COVID-19 Patients Using a Portable Quantum Dot Smartphone Device. *Nano Lett.* **2021**, *21*, 5209−5216.
(18) Jiang, N.; Tansukawat, N. D.; Gonzalez-Macia, L.; Ates, H. C.; Dincer, C.; Güder, F.; Tasoglu, S.; Yetisen, A. K. Low-Cost Optical Assays for Point-of-Care Diagnosis in Resource-Limited Settings. *ACS Sens.* **2021**, *6*, 2108−2124.
(19) Ince, B.; Sezgintürk, M. K. Lateral Flow Assays for Viruses Diagnosis: Up-to-Date Technology and Future Prospects. *TrAC, Trends Anal. Chem.* **2022**, *157*, No. 116725.
(20) Liu, Y.; Zhan, L.; Qin, Z.; Sackrison, J.; Bischof, J. C. Ultrasensitive and Highly Specific Lateral Flow Assays for Point-of-Care Diagnosis. *ACS Nano* **2021**, *15*, 3593−3611.
(21) Sotnikov, D. V.; Zherdev, A. V.; Dzantiev, B. B. Mathematical Model of Serodiagnostic Immunochromatographic Assay. *Anal. Chem.* **2017**, *89*, 4419−4427.
(22) Sotnikov, D. V.; Byzova, N. A.; Zherdev, A. V.; Dzantiev, B. B. Retention of Activity by Antibodies Immobilized on Gold Nanoparticles of Different Sizes: Fluorometric Method of Determination and Comparative Evaluation. *Nanomaterials* **2021**, *11*, No. 3117.
(23) Lisboa Bastos, M.; Tavaziva, G.; Abidi, S. K.; Campbell, J. R.; Haraoui, L. P.; Johnston, J. C.; Lan, Z.; Law, S.; MacLean, E.; Trajman, A.; Menzies, D.; Benedetti, A.; Khan, F. A. Diagnostic Accuracy of Serological Tests for Covid-19: Systematic Review and Meta-Analysis. *BMJ* **2020**, *370*, No. m2516.
(24) Panferov, V. G.; Safenkova, I. V.; Zherdev, A. V.; Dzantiev, B. B. Methods for Increasing Sensitivity of Immunochromatographic Test Systems with Colorimetric Detection (Review). *Appl. Biochem. Microbiol.* **2021**, *57*, 143−151.
(25) Panferov, V. G.; Safenkova, I. V.; Varitsev, Y. A.; Drenova, N. V.; Kornev, K. P.; Zherdev, A. V.; Dzantiev, B. B. Development of the Sensitive Lateral Flow Immunoassay with Silver Enhancement for the Detection of *Ralstonia Solanacearum* in Potato Tubers. *Talanta* **2016**, *152*, 521−530.
(26) Sotnikov, D. V.; Berlina, A. N.; Ivanov, V. S.; Zherdev, A. V.; Dzantiev, B. B. Adsorption of Proteins on Gold Nanoparticles: One or More Layers? *Colloids Surf., B* **2019**, *173*, 557−563.
(27) Sotnikov, D. V.; Byzova, N. A.; Zherdev, A. V.; Xu, Y.; Dzantiev, B. B. Silent Antibodies Start Talking: Enhanced Lateral Flow Serodiagnosis with Two-Stage Incorporation of Labels into Immune Complexes. *Biosensors* **2022**, *12*, No. 434.
(28) Lee, S. H.; Hwang, J.; Kim, K.; Jeon, J.; Lee, S.; Ko, J.; Lee, J.; Kang, M.; Chung, D. R.; Choo, J. Quantitative Serodiagnosis of Scrub Typhus Using Surface-Enhanced Raman Scattering-Based Lateral Flow Assay Platforms. *Anal. Chem.* **2019**, *91*, 12275−12282.
(29) Jia, J.; Ao, L.; Luo, Y.; Liao, T.; Huang, L.; Zhuo, D.; Jiang, C.; Wang, J.; Hu, J. Quantum Dots Assembly Enhanced and Dual-Antigen Sandwich Structured Lateral Flow Immunoassay of SARS-CoV-2 Antibody with Simultaneously High Sensitivity and Specificity. *Biosens. Bioelectron.* **2022**, *198*, No. 113810.
(30) Hou, F.; Bai, M.; Zhang, Y.; Liu, H.; Sun, S.; Guo, H. Fluorescent Immunochromatographic Assay for Quantitative Detection of the Foot-and-Mouth Disease Virus Serotype O Antibody. *Microchem. J.* **2020**, *155*, No. 104690.
(31) Roda, A.; Cavalera, S.; Di Nardo, F.; Calabria, D.; Rosati, S.; Simoni, P.; Colitti, B.; Baggiani, C.; Roda, M.; Anfossi, L. Dual Lateral Flow Optical/Chemiluminescence Immunosensors for the Rapid Detection of Salivary and Serum IgA in Patients with COVID-19 Disease. *Biosens. Bioelectron.* **2021**, *172*, No. 112765.
(32) Guzman, N. A.; Blanc, T.; Phillips, T. M. Immunoaffinity Capillary Electrophoresis as a Powerful Strategy for the Quantification of Low-Abundance Biomarkers, Drugs, and Metabolites in Biological Matrices. *Electrophoresis* **2008**, *29*, 3259−3278.
(33) Guzman, N. A.; Phillips, T. M. Immunoaffinity CE for Proteomics Studies. *Anal. Chem.* **2005**, *77*, 60A−67A.
(34) Luo, L.; Li, X.; Crooks, R. M. Low-Voltage Origami-Paper-Based Electrophoretic Device for Rapid Protein Separation. *Anal. Chem.* **2014**, *86*, 12390−12397.
(35) Moghadam, B. Y.; Connelly, K. T.; Posner, J. D. Two Orders of Magnitude Improvement in Detection Limit of Lateral Flow Assays Using Isotachophoresis. *Anal. Chem.* **2015**, *87*, 1009−1017.
(36) Moghadam, B. Y.; Connelly, K. T.; Posner, J. D. Isotachophoretic Preconcenetration on Paper-Based Microfluidic Devices. *Anal. Chem.* **2014**, *86*, 5829−5837.
(37) Gong, M. M.; Nosrati, R.; San Gabriel, M. C.; Zini, A.; Sinton, D. Direct DNA Analysis with Paper-Based Ion Concentration Polarization. *J. Am. Chem. Soc.* **2015**, *137*, 13913−13919.
(38) Panferov, V. G.; Ivanov, N. A.; Mazzulli, T.; Brinc, D.; Kulasingam, V.; Krylov, S. N. Electrophoresis-Assisted Multilayer Assembly of Nanoparticles for Sensitive Lateral Flow Immunoassay. *Angew. Chem., Int. Ed.* **2022**, DOI: 10.1002/anie.202215548.
(39) McNaught, A. D.; Wilkinson, A.; IUPAC. *Compendium of Chemical Terminology (the "Gold Book")*, 2nd ed.; Chalk, S. J., Ed.; Blackwell Scientific Publications: Oxford, 1997; Vol. *1669*, ISBN 0-9678550-9-8.
(40) Wu, Z.-Y.; Ma, B.; Xie, S.-F.; Liu, K.; Fang, F. Simultaneous Electrokinetic Concentration and Separation of Proteins on a Paper-Based Analytical Device. *RSC Adv.* **2017**, *7*, 4011−4016.
(41) Jack, A. D.; Hall, A. J.; Maine, N.; Mendy, M.; Whittle, H. C. What Level of Hepatitis B Antibody Is Protective? *J. Infect. Dis.* **1999**, *179*, 489−492.
(42) Bruce, M. G.; Bruden, D.; Hurlburt, D.; Zanis, C.; Thompson, G.; Rea, L.; Toomey, M.; Townshend-Bulson, L.; Rudolph, K.; Bulkow, L.; Spradling, P. R.; Baum, R.; Hennessy, T.; McMahon, B. J.

Antibody Levels and Protection After Hepatitis B Vaccine: Results of a 30-Year Follow-up Study and Response to a Booster Dose. *J. Infect. Dis.* **2016**, *214*, 16−22.
(43) World Health Organisation. *Guidelines on Hepatitis B and C Testing*; WHO, 2017; pp 1−170.
(44) Land, K. J.; Boeras, D. I.; Chen, X.-S.; Ramsay, A. R.; Peeling, R. W. REASSURED Diagnostics to Inform Disease Control Strategies, Strengthen Health Systems and Improve Patient Outcomes. *Nat. Microbiol.* **2019**, *4*, 46−54.
(45) Demonbreun, A. R.; Sancilio, A.; Velez, M. P.; Ryan, D. T.; Saber, R.; Vaught, L. A.; Reiser, N. L.; Hsieh, R. R.; D'Aquila, R. T.; Mustanski, B.; McNally, E. M.; McDade, T. W. Comparison of IgG and Neutralizing Antibody Responses after One or Two Doses of COVID-19 MRNA Vaccine in Previously Infected and Uninfected Individuals. *EClinicalMedicine* **2021**, *38*, No. 101018.
(46) Campbell, C.; Padmanabhan, N.; Romero, D.; Joe, J.; Gebremeskel, M.; Manjula, N.; Wohlstadter, N.; Wohlstadter, R.; Goodwin, P.; Quintero, L.; Debad, J.; Sigal, G.; Wohlstadter, J. Quantitative Serology for SARS-CoV-2 Using Self-Collected Saliva and Finger-Stick Blood. *Sci. Rep.* **2022**, *12*, No. 6560.
(47) Farci, P. Delta Hepatitis: An Update. *J. Hepatol.* **2003**, *39*, 212−219.
(48) Garfein, R. S.; Vlahov, D.; Galai, N.; Doherty, M. C.; Nelson, K. E. Viral Infections in Short-Term Injection Drug Users: The Prevalence of the Hepatitis C, Hepatitis B, Human Immunodeficiency, and Human T-Lymphotropic Viruses. *Am. J. Public Health* **1996**, *86*, 655−661.
(49) Chinnasamy, T.; Segerink, L. I.; Nystrand, M.; Gantelius, J.; Andersson Svahn, H. Point-of-Care Vertical Flow Allergen Microarray Assay: Proof of Concept. *Clin. Chem.* **2014**, *60*, 1209−1216.

https://doi.org/10.1021/acssensors.3c00130
ACS Sens. 2023, 8, 1792−1798